IEEE Access
Multidisciplinary | Rapid Review | Open Access Journal

Received April 23, 2016, accepted May 6, 2016, date of publication June 9, 2016, date of current version July 7, 2016.

Digital Object Identifier 10.1109/ACCESS.2016.2577553

A Wireless System for Monitoring Leakage Current in Electrical Substation Equipment

N. HARID[1], (Member, IEEE), A. C. BOGIAS[2], H. GRIFFITHS[1], (Member, IEEE), S. ROBSON[2], (Member, IEEE), AND A. HADDAD[2], (Member, IEEE)

[1]The Petroleum Institute, 2533, Abu Dhabi, United Arab Emirates
[2]School of Engineering, Cardiff University, Cardiff CF24 3AA, U.K.

Corresponding author: N. Harid (nharid@pi.ac.ae)

This work was supported by the U.K. Engineering and Physical Sciences Research Council under Grant EPSRC CASE/CAN/06/23.

ABSTRACT In this paper, the design and the development of a remote system for continuous monitoring of leakage currents and ground currents in high voltage electrical substations are proposed. Based on wireless local area network technology, the system can be used to monitor continuously a variety of plants within the substation and has low power consumption with inbuilt overvoltage protection. It consists of a transmitter module equipped with a data acquisition (DAQ) system connected to leakage current and voltage sensors, and a receiver module connected to a remote controller for data processing and storage. The principle of operation and the characteristics of the various components of the system are described. Validation tests have been used to verify its performance in three different test situations: A) laboratory monitoring of the leakage current and voltage of a distribution surge arrester; B) laboratory measurement of the leakage current of an outdoor insulator; and C) field monitoring of the earth current and potential rise of high-voltage tower. The measured results are in close agreement with those recorded directly through a DAQ card with fiber-optic and coaxial cable connected systems. Data processing is carried out at the receiving end so that the monitored parameter is displayed continuously or at specified time intervals. The operation of the system has been tested and proved resilient under high-frequency interference signals such as those generated by corona and surface discharges.

INDEX TERMS Continuous monitoring, data acquisition, high-voltage substation, insulator, leakage current measurement, solar power, surge arrester, wireless transmission, WLAN system.

LIST OF ABBREVIATIONS

ADC:	Analog to Digital Converter
AP:	*Access Point*
DAQ:	Data Acquisition
DSP:	*Digital Signal Processor*
EMI:	Electromagnetic Interference
FER:	*Frame Error Rate*
FPGA:	*Field Programmable Gate Array*
GDT:	*Gas Discharge Tube*
ISM:	*Industrial, Scientific and Medical*
MOSA:	*Metal Oxide Surge Arrester*
MOV:	*Metal Oxide Varistor*
MPPT:	*Maximum Power Point Tracker*
MV/HV:	*Medium Voltage/High Voltage*
SPI:	*Serial Peripheral Interface*
PCB:	*Printed Circuit Board*
SCADA:	*Supervisory Control and Data Acquisition*
TVS:	*Transient Voltage Suppressor*
UART:	*Universal Asynchronous Receiver Transmitter*
WLAN:	*Wireless Local Area Network*
WPAN:	*Wireless Personal Area Network*

I. INTRODUCTION

Electric power transmission and distribution systems are increasingly required to operate efficiently and reliably to guarantee both continuity and quality of supply. With many installations around the world using equipment that was installed decades ago and nearing the end of its service life, there is a need to monitor the condition of such equipment and possibly extend its service life without major system disruptions. This has prompted utilities to install plant and system monitoring devices in high-voltage substations, as well as in buried electric cables and on overhead power lines. Usually, such devices are used in conjunction with fiber optic links or hard-wired metallic cables to transmit information to a central monitoring point or SCADA system [1].

For upcoming smart grid applications, the number of such retrospectively-installed devices is expected to increase, and this poses the problem of large-scale deployment requiring considerable cost and installation effort. Among the practical challenges, for example, would be to ensure that such systems are immune from the effect of electric and magnetic fields generated in a high voltage installation, by providing appropriate insulation to withstand failure and breakdown. Wireless monitoring sensors, however, offer an attractive alternative to wired or fiber-optic systems for high-voltage equipment in substations, and have prospective application in wide-area monitoring of large power systems. Condition monitoring applications where data would be very expensive to acquire using traditional wired communication systems, could benefit from the use of wireless sensors. In this case, wireless sensors would help avoid effects of ground potential rise and reduce the difficulty and cost of installing wiring across substation yards. Wireless sensor systems can play a role in substation condition monitoring, but this role must take into account the realities of wireless vulnerabilities to EMI, path obstacles, scattering, congestion of the limited frequency spectrum, and other factors such as the number of access points (AP) required. A feasibility study on deploying wireless technologies in high voltage substations has shown that WIFI technology performs satisfactorily in terms of substation coverage, signal propagation, security and data rate [2]. High voltage substations present special challenges in this respect due to the presence of many metallic structures causing multiple reflections, diffractions and scattering. It has been argued [3] that WLAN, IEEE 802.11b/g and WPAN can be successfully applied for monitoring high-voltage substations, electric power lines and plant. Some authors proposed wireless data acquisition systems for measuring high-frequency signals such as transient EMI signals [4] and partial discharge signals [5]. In [6], a wireless surge arrester leakage current sensor, based on the ZigBee protocol, capable of transmitting over a distance of 400 m was developed and tested in a 230kV substation. The authors of [7] propose a wireless capacitive sensor for monitoring voltage variations of MV/HV plant using ZigBee technology. Other monitoring solutions have also been proposed for use with electrical plant [8].

In addition to noise and external interference, wireless DAQ systems need to be immune to information loss errors and unauthorized access to data. This can be resolved with the selection of a wireless technology that provides robust security, both in terms of data encryption and network connectivity. Issues of overloaded bandwidth, disruption of the wireless signal due to electromagnetic interference need to be carefully examined. When sensors and wireless transmitters are mounted on or near high-voltage equipment, high-frequency noise and interference can affect their performance. For example, previous experimental results [9] showed a correlation between the breakdown events in vacuum and SF_6 and a sharp decline in the data rate of 802.11b wireless devices. In [10], the authors demonstrated that WLAN sensors can be used in substations for monitoring and metering applications, despite transmission delays incurred due to noise, which were within allowable limits. The authors of [11] investigated the effect of high impulsive transients on the wireless transfer performance of WiFi and ZigBee communications, and concluded that WiFi provides higher immunity to such transients compared with ZigBee. Impulsive noise effects on WLAN performance have also been reported in a laboratory environment [12].

This paper describes the design, development and testing of a microcontroller-based wireless data acquisition system for monitoring leakage current and voltage in high-voltage substation electrical equipment. The system is a solar-powered device with back-up battery storage. A design prototype was initially tested in the laboratory with relatively short transmission distances [13], and later improved as a self-powered device [14]. This work builds on this design by introducing improvements in data acquisition algorithms, extending the experimental validation to an outdoor test facility, and demonstrating its transmission performance with and without partial discharge interference. The results obtained using the proposed system are compared with those recorded directly through a wired data acquisition system. The device could find application both in line-mounted equipment monitoring such as line voltage, line current and temperature monitors and as well as ground-mounted equipment such as leakage current monitors in substations. The proposed method is easier to implement and provides a cheaper alternative compared with existing methods that use wired communication systems, while achieving similar data transmission performance. It is also expected to be less susceptible to high-voltage interference effects such as electromagnetic coupling and ground potential rise.

II. PROPOSED SYSTEM DESCRIPTION

A simplified operational block diagram of the proposed system is shown in Figure 1. The continuously-measured voltage and current signals obtained from sensors installed at the equipment to be monitored are fed into a WLAN-IEEE 802.11b/g transmitter/receiver block (WLAN Tx/Rx). The measured signals are pre-conditioned as described in section 3 before they are transmitted to a remote access point and a control station (personal computer). The LabVIEW^{TM} platform is used for real time continuous monitoring and data processing. The system features two-way communication capability which enables synchronized data

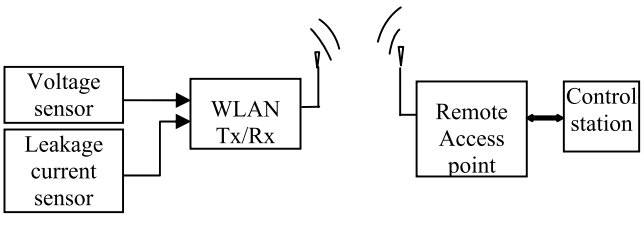

FIGURE 1. Simplified block diagram of the WLAN system.

transfer and acquisition. The design steps, the details of the various circuitry and the characteristics of the different components forming the complete system are described in [15].

A. WLAN TX/RX TRANSMISSION BLOCK COMPONENTS

The transmitter block consists of four main components: the signal conditioning component, the microcontroller, a transceiver module and a solar power supply with energy storage. The input conditioning component contains an external ADC, low-pass filters and a surge protection unit. Figure 2(a) shows the schematic block diagram of the different components with their power/control interconnections and interfaces. Figure 2(b) shows the constructed prototype; the components are PCB mounted and the overall assembly is placed in a metallic enclosure with two BNC connectors, the wireless antenna and the battery pack.

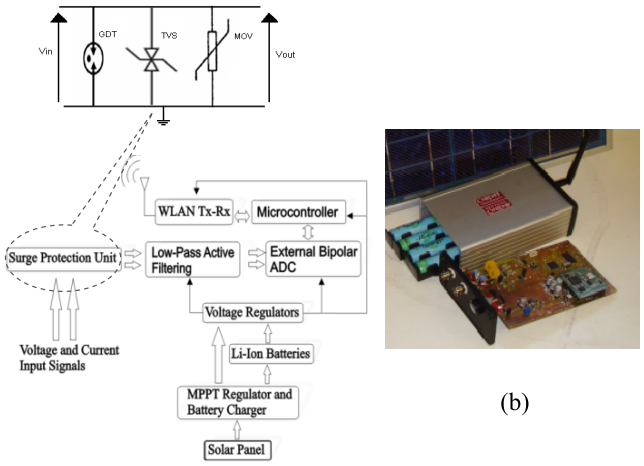

FIGURE 2. (a) Block diagram of the transmission block of the WLAN system, (b) The wireless system with its enclosure.

B. SIGNAL CONDITIONING CIRCUIT

The objective of the proposed WLAN system is to measure AC signals on two channels, with a 14-bit resolution and a sampling rate of at least 80 kHz. A 2-channel bipolar, ±5 V, 500 kHz, ADC was chosen to avoid using additional level shifting circuitry required to interface an AC signal to a unipolar ADC. Two low-pass filters which use multiple operational amplifiers were required in each channel for anti-aliasing purposes. To isolate the impedance of the sensor from that of the anti-aliasing filter, a buffering op-amp was required before the input of each of the filter circuitry.

The inputs to the analogue component were fed directly from the voltage and current sensors. A three-stage protection circuit consisting of a GTD, TVS and MOV was used for protecting the WLAN sensor against surge overvoltages. The circuit diagram of this protection system is shown in the enclosure of Figure 2(a), and it was developed to combine the high energy absorption capacity of the GDT with the fast response of the MOV and TVS.

C. WLAN MODULE

The WLAN module is composed of a MatchPort MP1002000G-01 wireless transceiver, which receives data through its UART port and converts into TCP/IP packets and finally into 802.11 packets, ready for wireless transmission. It is a dual processor communication device that enables both 802.11b/g wireless connectivity. It has a maximum data throughput of 921.6kbps and, with an external 2dBi antenna fitted on this trial prototype, it is able to transmit over a range of 100 meters, but the range can be extended by using a high gain directional antenna. Information received from the microcontroller is encapsulated using the TCP/IP protocol by the WLAN module to ensure the integrity of the data prior to transmission. The WLAN module supports 256-bit Advanced Encryption Standards (AES) for end-to-end secure data transfer, and has a maximum power consumption of 740mW. At the control station, the remote access point (AP) is programmed to convert the TCP/IP packets back into RS-232 data format before feeding this information into the LabVIEW^{TM}program, which processes and compiles data into a user-friendly format for the developmental version.

1) MICROCONTROLLER

A 16-bit high performance, low-power microcontroller with on-board serial communication module is used here to control the data acquisition process. The use of a separate microcontroller has the advantage of allowing the user to choose the programming language as well as the microprocessor that best suits the needs of the application under consideration. For the given sampling rate and ADC resolution, the PIC24HJ256GP210 microcontroller was used. It has a 16-kB of RAM memory, and its CPU has 16-bit data and 24-bit address paths. It was set to operate at its maximum speed of 40MHz. This speed was considered adequate and removed the need to move to faster DSP ICs or more complex FPGAs and microcontroller hybrid designs. The maximum power consumption of the chosen microcontroller, when it is running at its maximum operating speed, was anticipated to be in the few hundreds of mW. A parallel memory IC was chosen based on its fast speed and adequate storage size of at least 1 second worth of acquired data. The microcontroller, which receives waveform data via a Serial Peripheral Interface (SPI), has full control of the analogue-to-digital conversion by triggering the ADC at the appropriate sampling rate. The SPI was programmed to have a maximum data rate of 1,250kbps and communicate in 16-bit long packets. Data is stored sequentially in an internal memory buffer, and subsequently transmitted in the RS-232 format.

2) POWER SUPPLY MODULE

The system is designed to be self-powered using solar power as the main source, with energy storage facility for night usage and low-irradiation operation. The choice of solar power was to ensure that a sustained energy supply is available for continuous monitoring of the leakage current, without the need for battery replacement.

Alternative methods can also be considered for supplying energy to the system such as energy harvesting from the magnetic field or electric field in the high voltage busbars using inductive or capacitive devices respectively. Solar power is common for powering wireless networks, and many devices have been proposed in the literature [16]–[20]. This system uses a semi-crystalline silicone solar panel backed up with a rechargeable battery pack, and can typically generate 20W peak power, with an output voltage of 16.8V and a current of 1.19A under standard irradiance and temperature conditions. The battery charger is a Linear Technology LT3652 monolithic step-down (buck) type that operates over an input range of 4.95V to 16.8V. The charger incorporates an MPPT regulator to optimize power output under varying light irradiance conditions and adjusts the solar panel output between 5.6V and 8.4V, according to the operational requirements of the battery. The battery pack consists of an array of rechargeable Lithium-Ion batteries each with normal operating range between 2.8V and 4.2V. These batteries have high-energy density and long discharge time-constant, and can provide full power continuously for 19 hours during low- or no-irradiance periods.

The battery charger was tested with a solar test facility using a halogen-tube array light source. The measured voltage and current profiles during the charging time are shown in Figure 3, with the WLAN system in non-transmitting mode. This voltage reaches 8.2 V when the battery is fully charged, and only half an hour charging time is required to reach 90% battery voltage. The charging time may vary depending on actual irradiance and operational state of the WLAN module. The maximum power consumption of the WLAN Tx/Rx block has been experimentally measured and was found not to exceed 2.1W when it is acquiring and transmitting data.

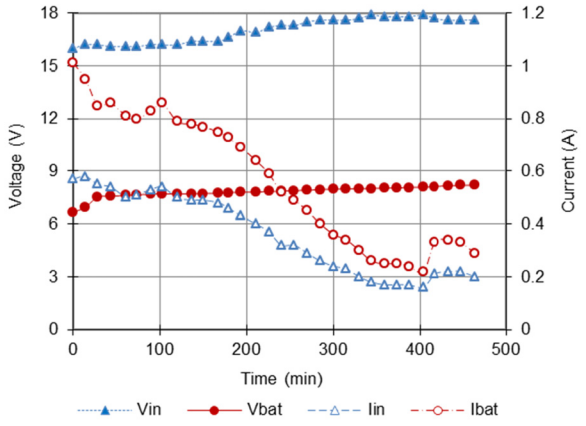

FIGURE 3. Battery voltage and current profiles over entire charging time Vin, Iin: Input voltage and current from solar panel, Vbat, Ibat: Battery voltage and current.

3) REGULATED VOLTAGE SUPPLY

To provide stable supply voltage to the WLAN block and ensure reliability of transmitted data, voltage output regulators were used. A step down DC/DC converter model LT1933 was used to provide a regulated voltage of 3.3V at 500mA to supply the microcontroller and the WLAN module. When operating within the voltage range of the Li-Ion battery pack, this converter has an efficiency of about 80%. For the active filtering and ADC circuits, a buck/boost type MCP1253 DC/DC converter is used to generate a regulated 5V output voltage, and a TC1121 voltage converter is used to provide a negative −5V output voltage for the ADC. These converters are suitable for use in applications requiring low noise and high efficiency.

III. EXPERIMENTAL VALIDATION OF THE PROPOSED SYSTEM

The developed system was tested using three specific condition monitoring applications for surge arresters, polluted insulators and earthing systems. The cost of the proposed system is estimated to be equivalent or less than that of a wired monitoring system since it uses inexpensive wireless equipment requiring low installation cost, with no requirement for cabling.

A. MONITORING OF SURGE ARRESTER LEAKAGE CURRENT

Surge arresters have highly non-linear characteristics and are widely used for protecting high-voltage substation equipment [21], [22]. Condition monitoring of these devices can be achieved by measuring the on-line leakage current. Leakage current combined with signal processing techniques is a reliable diagnostic tool which provides useful information on the state of degradation the surge arrester [23], [24]. Commercial devices are available for condition monitoring of surge arresters [25], [26], but these are not ideal for continuous monitoring applications. Although they can be self-powered, they rely on radio communications and require the presence of an operator in-situ to download the measured data for post-processing.

To validate the ability of the WLAN system to perform on-line continuous monitoring, tests were carried out in a high-voltage laboratory using the arrangement shown in Figure 4. A high voltage transformer generates a controlled AC voltage applied to a metal oxide surge arrester (MOSA) having a rated voltage of 15kV and a nominal discharge

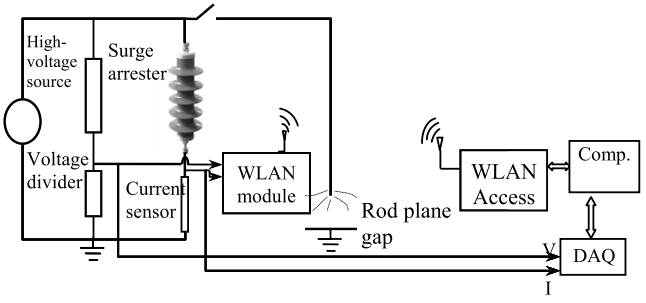

FIGURE 4. Experimental validation set-up for surge arrester leakage current measurement.

current of 10kA. The voltage was measured using a mixed resistive-capacitive voltage divider of 4750:1 ratio, and the total leakage current of the surge arrester was measured using a suitably selected resistive sensor. Both the voltage and leakage current signals were connected to the inputs of the WLAN module and, for the measurement validation, also to a Data Acquisition (DAQ) card, via coaxial cables, as can be seen in Figure 4. The DAQ card has a 16-bit resolution, +/−10V input voltage range and 20 kHz sampling rate.

1) LEAKAGE CURRENT MEASUREMENT RESULTS

Measurements were carried out at several voltage levels up to the arrester rated voltage. Examples of the voltage and current waveforms recorded with a 12 kVrms applied voltage using the WLAN sensor and directly through the DAQ card are shown in Figures 5(a) and 5(b) respectively. In the low-conduction regime, the surge arrester has a very high resistance, and the leakage current consists of a small and predominantly capacitive current. This behaviour is well reproduced by the WLAN sensor which shows signals very close in magnitude and shape to those measured with the DAQ card. The phase difference between the voltage and current signals was also accurately measured. The phase shift between the DAQ signal and WLAN signal is due to transmission delay incurred in the WLAN module and access point.

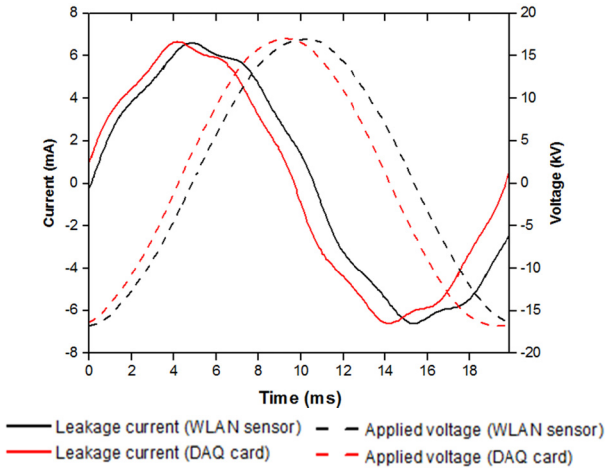

FIGURE 5. Example of applied voltage and leakage current signals, surge arrester in non-conduction mode.

2) LEAKAGE CURRENT MEASUREMENT IN THE PRESENCE OF PARTIAL DISCHARGE

Partial discharges such as corona from live conductors and equipment terminals, radiate high-frequency signals and may affect the WLAN system performance. To simulate such environment, a rod-plane electrode gap was used, with the tip of the rod sufficiently sharp to initiate air discharge at the test voltage (Figure 4). Under these conditions, the waveforms measured simultaneously with the WLAN system and the DAQ card are shown in Figure 6 for an applied voltage

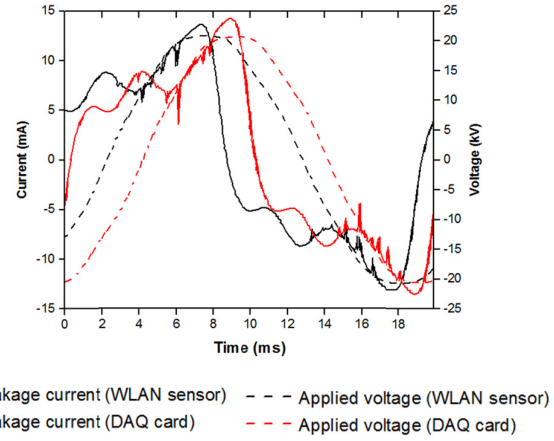

FIGURE 6. Measured voltage and current signals, arrester in conduction mode with corona discharge.

of 14.5 kVrms. At this voltage, the surge arrester exhibits a higher leakage current with a large resistive component. Similar to the DAQ card, the WLAN system is able to reproduce the main features of the leakage current and the corona discharge pulses superimposed on the current signal, which occur when the voltage exceeds a threshold value on the positive and negative half cycles. Slight differences between the WLAN system and the DAQ card signals could be attributed to differences in the resolution and sampling rates of the two systems, in addition to the transmission delay causing the phase shift. In practice, bad weather conditions usually intensify the corona discharge and the pulse amplitude may exceed the input voltage limit of the WLAN module, which may activate the overvoltage protection circuit. Immunity from high-frequency partial discharge noise is an important feature for long term continuous monitoring.

B. MONITORING LEAKAGE CURRENT AND DISSIPATED POWER OF POLLUTED INSULATORS

The surface conduction current on outdoor insulators is a good measure of insulator surface condition and can be used to detect incipient faults and defective insulators. In heavily polluted areas, the conduction increases due to contamination by wetted salts and other conducting particles. The installation of leakage current sensors on lines and substations located in these areas can be very useful for monitoring the pollution severity and the surface condition of insulators [27]–[29].

1) POLLUTED INSULATOR TEST PROCEDURE

Experiments were carried out using a set-up illustrated in Figure 7 on two ceramic outdoor insulators placed in a fog chamber; a healthy insulator and a defective insulator of the same design. Artificial pollution was applied by immersion of the insulators in a salt solution according to recommended IEC 60507 standard procedures [30]. The applied voltage and the surface leakage current were monitored with both the

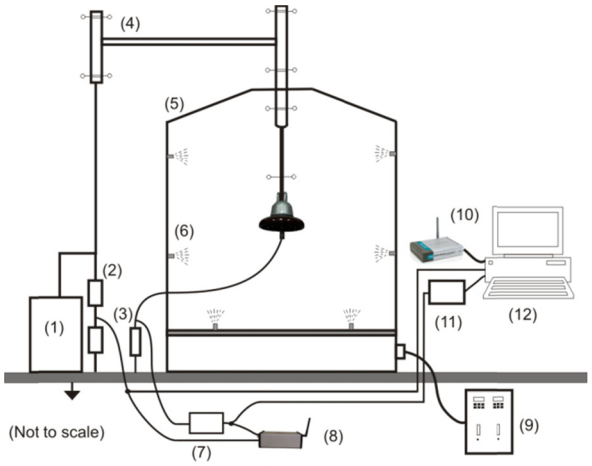

FIGURE 7. Test arrangement for outdoor polluted insulator 1: High-voltage source, 2: Mixed resistive-capacitive HV divider, 3: Variable resistance, 4: High-voltage conductor and stress control rings, 5: Fog chamber, 6: Spray nozzle, 7: Surge protection box, 8: WLAN module, 9: Fog/rain control unit 10: WLAN Access point, 11: Surge protection and low pass filter, 12: PC containing DAQ card.

WLAN system and the same DAQ card, for a continuous test period of 10 mins. The data, such as rms conduction current, power dissipation and accumulated energy at the remote end were calculated from the voltage and current information to explore indicators of insulator surface condition.

2) RESULTS OF INSULATION MONITORING TEST

At the beginning of the test, small surface discharges start to occur and the leakage current is mainly resistive due to the conduction of the wet pollution layer. As the test progresses, the heating due to current flow creates dry-bands where conduction stops. These dry bands are bridged by arcs as the voltage builds up during each half cycle.

Figures 8 (a) and 8(b) show examples of the leakage current waveforms for the healthy and defective insulators measured using both the WLAN system and DAQ card for an applied voltage of 11 kV. This test voltage is the highest voltage that the insulator is required to withstand under normal operating conditions. It can be seen that the waveforms measured by the WLAN system are identical to those measured by the DAQ card after the transmission delay is suppressed, and were within less than 1% of those measured by the DAQ card. The sharp rise in the leakage current occurring at voltage minima and maxima is attributed to dry-band arcing, with the defective insulator showing much larger current peaks.

3) MONITORING OF LEAKAGE CURRENT AND POWER OVER A LONG PERIOD

Continuously monitored leakage current and applied voltage for a period of 10 mins were processed to give the current and voltage magnitudes (rms and peak values), their total harmonic distortion, the average dissipated power and the accumulated energy of the surface discharges over the test period. The average dissipated power and the accumulated

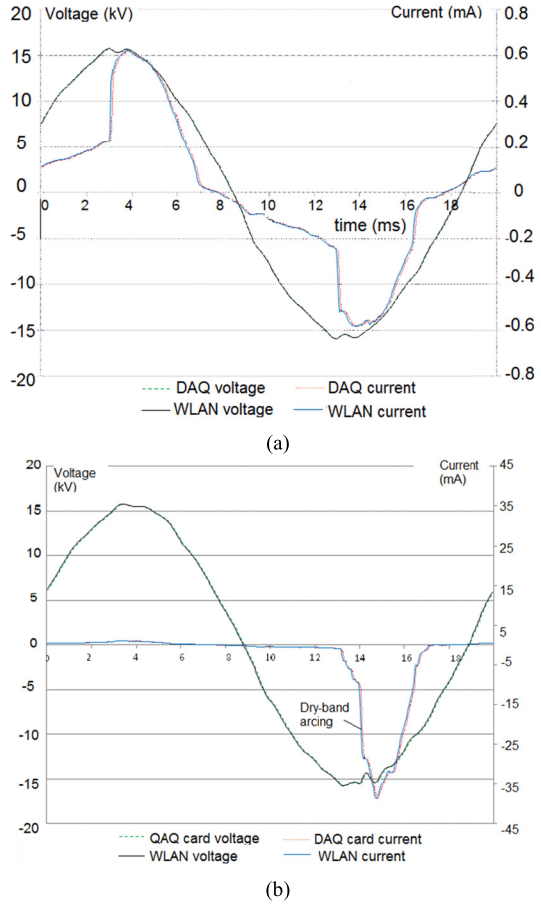

FIGURE 8. Examples of measured voltage and leakage current signals at an applied voltage of 11 kV. (a) healthy insulator (b) defective insulator.

energy can be used as indicators of insulator surface heating and material degradation. Figure 9 shows examples of monitored peak current and average dissipated power for both insulators. From the figure, a clear distinction can be observed between the healthy and defective insulator results

Surface discharges that occur on the surface of the defective insulator result in current peak values that are up to 100 times larger compared with those of the healthy insulator. The peak of the leakage current and the average dissipated power show a decreasing trend with time for the healthy insulator as the discharges become more sporadic, indicating a slowdown in surface current activity due to pollution being washed off the insulator surface. This is not the case with the defective polluted insulator. Discharge currents with large peak values continue to occur frequently throughout the test, although decreasing slightly towards the end of the test.

To observe the variability of the measured data, a data sample of 150 points was taken, for which the rms values were averaged over a period of 3000 ms for a constant applied voltage of 6.7 kV. Table 1 shows the statistical data for this sample. The WLAN system shows slightly higher variance than the DAQ card, but is able to trace the leakage current with good accuracy. In practical operation, averaging is made over much longer time scales, which improves accuracy.

TABLE 1. Leakage current statistical data.

	Sample size	Min (mA)	Max (mA)	Average (mA)	Standard Deviation (mA)
DAQ	150	0.99	9.48	3.06	2.15
WLAN	150	0.95	11.84	4.36	2.58

C. FIELD TEST: MONITORING OF EARTH CURRENT AT TRANSMISSION TOWER

In high-voltage substations, earth currents continuously flow to ground through earthing grids, towers, earth wires and cable sheaths. Monitoring of these earth currents could help in assessing the performance and the integrity of the earthing system, which is essential for safety of people and protection of equipment. Presently, the monitoring of the continuously-flowing current is not performed by utilities, and earthing tests only provide the system earth impedance. Under normal operating conditions, it is possible to monitor the current flowing in the earth grid through earth wires simultaneously with the potential with respect to remote earth.

An earthing grid monitor that uses this principle has been developed and tested on operational substations [31]. This method can be used to monitor the system earth impedance, a key parameter for inspecting the earthing system integrity.

The proposed wireless sensor has been used to monitor remotely the earth impedance of a transmission tower at an outdoor location using this principle. A variable frequency source injects current into four 3m-long buried tower footings of a 275kV transmission test tower base arranged in a 7.5m×7.5m square to simulate the natural earth leakage current or that of an active low voltage current injection test system. (Figure 10).

The traces of current and voltage sensors are measured using a CT and a differential voltage probe, which are then fed to the WLAN transmitter input terminals. During the experiment, the WLAN transmitter was operated from the batteries, and the receiver was located 60m away from the tower base. Figure 11 shows values of the tower base impedance (V_{rms}/I_{rms}) derived from measured data and displayed over of a duration of 150 cycles. The measured average impedance is 22.4Ω over the measurement period, but the averaging time can be adjusted for optimal memory and energy usage. Breaks in the earthing system integrity were simulated by suddenly disconnecting one or more footings.

Figure 12 illustrates the monitoring of the tower base earthing integrity over a 10-min period when one and two of the tower footings were disconnected. An increase in tower base impedance of 36% and 72% is seen when one footing and two footings are disconnected at times t=70.2 s and t=93.5 s respectively. Such a large increase is synonymous of a break in the earthing system, but other system defects such as poor contacts or high-resistance bonding between earthing system components would show a smaller change in impedance magnitude. Measurements carried out with a 200MHz oscilloscope and a conventional earth instrument gave identical results.

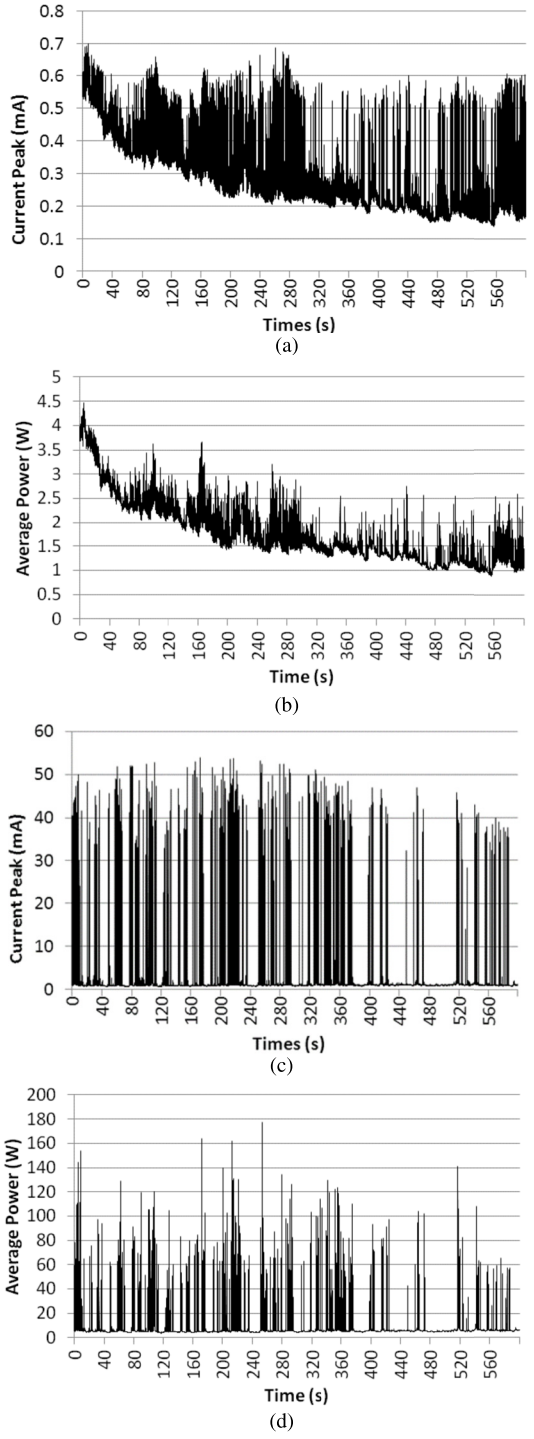

FIGURE 9. Monitoring of leakage current and average dissipated power of 11kV polluted insulators using WLAN system, (a, b) leakage current and dissipated power, healthy insulator, (c,d) leakage current and dissipated power, defective insulator.

IV. WIRELESS TRANSMISSION PERFORMANCE OF THE WLAN SYSTEM

The wireless performance of the WLAN module and access point was tested both in the outdoor test field described in Section 4 with no wireless networks detectable in the vicinity and in the high voltage laboratory, where a relatively large

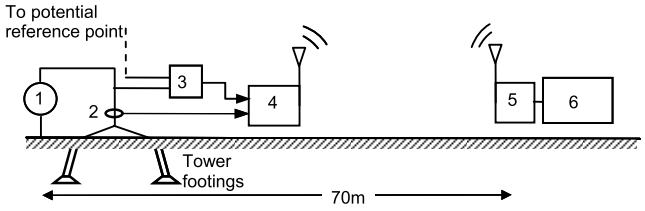

FIGURE 10. Outdoor test set-up for measurement of earth current and earth potential rise 1: AC source, 2: Current sensor, 3: Voltage sensor, 4: WLAN module, 5: Access point, 6: control station.

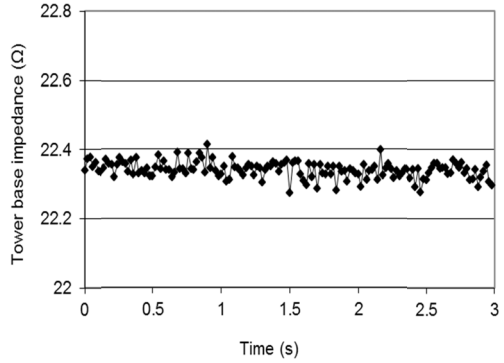

FIGURE 11. Measured tower base impedance using WLAN system.

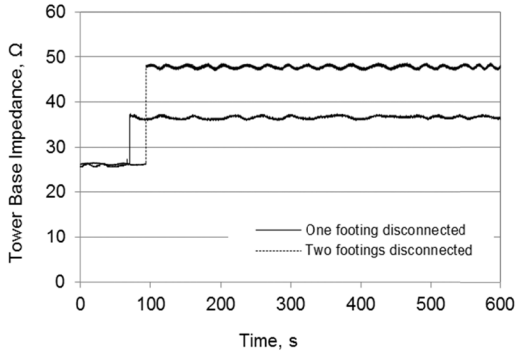

FIGURE 12. Monitoring the earth impedance of tower base footings using the WLAN sensor: effect of break in earthing system.

number of 802.11 networks using the 2.4GHz spectrum exist. For the field test set-up, The WLAN sensor, which was controlled by a laptop computer, was placed at a distance of 60m from a DI-524 link. An AirPcap Tx USB adapter [32] was used in conjunction with the protocol analyzer Wireshark to capture wireless 802.11b/g traffic on the channel the WLAN Sensor was transmitting onto. The Cascade Pilot PE analyzer was used to carry out traffic analysis, examine channel usage, errors and retransmissions. A Wi-spy 2.4x USB spectrum analyzer [33] was used in conjunction with the spectrum analysis software Chanalyzer Pro to measure the 2.4-GHz ISM spectrum, enable the discovery of noisy channels, identify interfering devices and enable optimum WLAN speed and performance. The computer associated with the WLAN sensor and the USB adapters and software described above will be referred to as the Wi-Fi interference monitor. At the receiver location, a 10dBi directional antenna was placed at a height of about 2.6m, and connected via a low loss coaxial cable to the DI-524 access point, which is connected to a second computer that controls the triggering and interruption commands for the wireless transmission.

The performance was measured in the 2.4-2.5 GHz spectrum over a 10-minute transmission period, for 802.11 channels 1, 6 and 11, which are considered non-overlapping channels. In the high voltage laboratory, the wireless performance test was carried out both with and without high voltage energization, with a distance of 2.3m between the Wi-Fi interference monitor and the access point.

Figures 13 shows selected examples of normal traffic and retransmitted data exchanged between the DI-524 access point and the WLAN sensor, recorded on channel 11 in both the field and the laboratory. Both cases show a steady data throughput, averaging about 720 kBps and 780 kBps respectively, with low re-transmitted data throughout the test. In the laboratory test, the normal traffic waveform experiences a small drop about 360 s into the measurement, corresponding to a small dip in the access points signal strength from -37dBm to -44dBm. When a large number of highly active interfering access points exist, the retransmitted data waveform would exhibit more pronounced spikes.

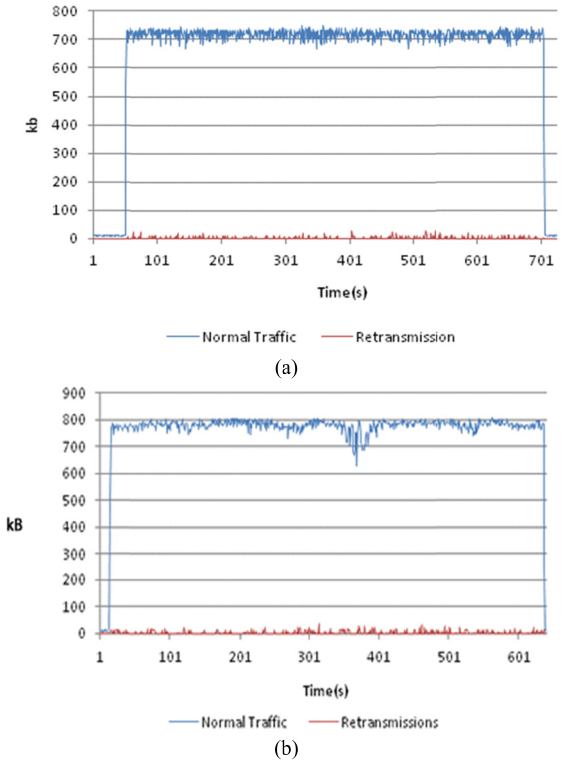

FIGURE 13. Normal traffic and retransmissions between WLAN module and DI-524 access point during laboratory test. (a) Channel 1 (b) Channel 6.

A. ANALYSIS OF WIRELESS TRAFFIC

The Wi-Fi interference monitor was used in this work to measure the frame error rate (FER), the channel utilization,

the number of access points and the total transmitted packets. The field tests, used as a benchmark, show a low FER for all three channels used. The analysis of the WLAN performance test results is summarized in Table 2. The differences in magnitude of the FERs for the three channels used, is largely affected by the amount of wireless data transmitted by external access points and stations. The more external wireless data is transmitted, the higher is the FER. In the high-voltage laboratory test, the WLAN system suffers the highest FER on channel 6 compared with other channels. The channel utilization is derived from a variable used by the WI-Spy analysis software to evaluate the usage of an 802.11 channel over a period of time, and which measures how much RF activity is affecting the channel. It is weighted so that signals near the center of the channel have a greater effect on the utilization score. It can be seen that the channel utilization during the laboratory test where more RF activity is present is higher than that measured during the field test. The 'access points detected' show all the access points identified during the entire 2.4GHz spectrum measurement period, and the values shown include the DI-524 access point used during the test. As expected, a much larger number of access points with equally large transmitted packets were detected in the high-voltage laboratory test, which affects the FER accordingly.

TABLE 2. Traffic data between WLAN sensor and access point during performance tests.

	Field test			Lab test			
Channel	**1**	**6**	**11**	**1**	**6**	**6***	**11**
FER (%)	0.17	0.49	0.21	1.48	1.74	1.57	0.33
Channel utilisation (%)	2.6	2.7	2.6	3.8	4.2	3.8	3.7
Access points	3	2	1	10	20	8	8
Packets transmitted	2297	3751	2375	19834	23958	16620	1986

*: with HV equipment energized.

There was no evidence to suggest that interference produced by energized high voltage equipment affects the wireless performance of the WLAN sensor. The 2.4-2.5GHz frequency content during the high voltage insulator tests contains no signals other than 802.11 detected access points.

B. WIRELESS TRANSMISSION RATE

Table 3 shows the percentage of data transmitted at each transmission rate on channels 1, 6 and 11 measured by the Wi-Fi interference monitor. On channels 1 and 11, while most of the data used the highest possible 802.11 transmission rate, a significant portion of the data exchanged between the WLAN module and access point has taken place at a rate of 48 Mbps or lower. The rate adaptation is more severe during the test on channel 6 compared to those on channels 1 and 11. This is an indication that a higher gain antenna for the WLAN module or the access point or both, would be advantageous. A low signal strength has the effect of dropping the wireless data transmission rate. This causes an increase in the receiving sensitivity in both the WLAN module and access point.

TABLE 3. Percentage of data transmitted at each transmission rate on channels 1, 6 and 11.

Test location	Channel	Transmission rate (Mbit/s)			
		54	48	36	24
Field	1	87.4%	12.6%	0.0%	0.0%
	6	65.2%	25.7%	8.6%	0.5%
	11	86.9%	13.0%	0.0%	0.0%
HV Lab	1	88.5%	11.4%	0.1%	0.0%
	6	81.5%	6.8%	6.0%	4.0%
	11	99.97%	0.0%	0.0%	0.0%

V. CONCLUSION

This paper has demonstrated the feasibility of a novel wireless condition monitoring system for application in high voltage electrical substations. The system can be used as a standalone device or part of a multi-sensor network to measure leakage current and voltage in a variety of equipment. It can be configured to provide continuous data acquisition at 80 kHz sampling rate on two channels and monitor specific quantities such as leakage current peak and r.m.s values, power dissipated, and accumulated energy at regular time intervals. It has been successfully tested in three different monitoring applications: (A) for monitoring the leakage current of a surge arrester, (B) monitoring the surface conduction current of polluted insulators and (C) monitoring the earth current flowing through the footings of a high-voltage tower. The measured results were validated against those measured directly using a wired data acquisition card, and showed excellent agreement. The effect of high-frequency interference signals generated by electrical discharges on the performance of the device was examined. Comparative tests were also performed to determine the wireless sensor immunity to interference within a high voltage laboratory environment and in an outdoor test facility. Analysis of wireless traffic measurements confirm that no interferences which might affect 802.11 networks are emitted from high voltage sources. Further work is required to improve accuracy, account for transmission delays, and extend the application to multiple sensors.

REFERENCES

[1] *IEEE Standard for SCADA and Automation Systems*, IEEE Standard C37.1-2007, 2007.

[2] L. A. Basile, S. Riendeau, H. Bertrand, and J. Béland, "The deployment of wireless networks in high voltage substations: A feasibility study," in *Proc. IEEE Elect. Power Energy Conf. (EPEC)*, London, ON, Canada, Oct. 2012, pp. 46–50.

[3] F. Cleveland, "Use of wireless data communications in power system operations," in *Proc. IEEE PES Power Syst. Conf. Expo. (PSCE)*, Oct./Nov. 2006, pp. 631–640.

[4] Y. Wang, F. A. M. Mir, and W. H. Siew, "Digital wireless data acquisition system for measurement in high voltage substations," in *Proc. IEEE Power Eng. Soc. General Meeting*, Jun. 2006, pp. 1–6.

[5] P. C. Baker, M. D. Judd, and S. D. J. McArthur, "A frequency-based RF partial discharge detector for low-power wireless sensing," *IEEE Trans. Dielectr. Electr. Insul.*, vol. 17, no. 1, pp. 133–140, Feb. 2010.

[6] E. C. T. Macedo, J. G. Alira, E. G. Costa, and M. J. Maia, "Wireless sensor network applied to ZnO surge arrester," in *Proc. Int. Symp. High Voltage Eng.*, Hanover, Germany, 2011, p. 396.

[7] R. Moghe, A. R. Iyer, F. C. Lambert, and D. M. Divan, "A low-cost wireless voltage sensor for monitoring MV/HV utility assets," *IEEE Trans. Smart Grid*, vol. 5, no. 4, pp. 2002–2009, Jul. 2014.

[8] L. Juan, J. Shaohua, W. Yirong, and W. Hui, "Online insulation monitoring system of high-voltage capacitive substation equipment based on WSN," in *Proc. China Int. Conf. Electr. Distrib. (CICED)*, Sep. 2010, pp. 1–6.

[9] X. Wang *et al.*, " Reliability test of using 802.11b technology in switchgear for measurement and control," in *Proc. Int. Conf. Power Syst. Technol.*, Oct. 2006, pp. 1–6.

[10] P. P. Parikh, T. S. Sidhu, and A. Shami, "A comprehensive investigation of wireless LAN for IEC 61850-based smart distribution substation applications," *IEEE Trans. Ind. Informat.*, vol. 9, no. 3, pp. 1466–1476, Aug. 2013.

[11] A. Abdrabou and A. M. Gaouda, "Uninterrupted wireless data transfer for smart grids in the presence of high power transients," *IEEE Syst. J.*, vol. 9, no. 2, pp. 567–577, Jun. 2015.

[12] Q. Shan *et al.*, "Laboratory assessment of WLAN performance degradation in the presence of impulsive noise," in *Proc. Int. Wireless Commun. Mobile Comput. Conf. (IWCMC)*, Crete Island, Greece, Aug. 2008, pp. 859–863.

[13] A. C. Bogias, N. Harid, A. Haddad, and H. Griffiths, "Wireless data acquisition system for high voltage substations," in *Proc. 16th Int. Symp. High-Voltage Eng.*, Cape Town, South Africa, 2009, pp. 1–5.

[14] N. Harid, "A solar-powered wireless data acquisition system for monitoring electrical substations," in *Recent Advances in Circuits, Communications and Signal Processing*, A. Said, C. H. H. Tang, and S. Oprisan, Eds. WSEAS Press, 2013, p. 23.

[15] A. C. Bogias, "A wireless 802.11 condition monitoring sensor for electrical substation environments," Ph.D. dissertation, School Eng., Cardiff Univ., Wales, U.K., 2012.

[16] V. Raghunathan, A. Kansal, J. Hsu, J. Friedman, and M. Srivastava, "Design considerations for solar energy harvesting wireless embedded systems," in *Proc. 4th Int. Symp. Inf. Process. Sensor Netw. (IPSN)*, Apr. 2005, pp. 457–462.

[17] D. Dondi, A. Bertacchini, D. Brunelli, L. Larcher, and L. Benini, "Modeling and optimization of a solar energy harvester system for self-powered wireless sensor networks," *IEEE Trans. Ind. Electron.*, vol. 55, no. 7, pp. 2759–2766, Jul. 2008.

[18] Y. Li, H. Yu, B. Su, and Y. Shang, "Hybrid micropower source for wireless sensor network," *IEEE Sensors J.*, vol. 8, no. 6, pp. 678–681, Jun. 2008.

[19] C. Alippi and C. Galperti, "An adaptive system for optimal solar energy harvesting in wireless sensor network nodes," *IEEE Trans. Circuits Syst. I, Reg. Papers*, vol. 55, no. 6, pp. 1742–1750, Jul. 2008.

[20] J. W. Kimball, B. T. Kuhn, and R. S. Balog, "A system design approach for unattended solar energy harvesting supply," *IEEE Trans. Power Electron.*, vol. 24, no. 4, pp. 952–962, Apr. 2009.

[21] *Surge Arresters- Metal-Oxide Surge Arresters Without Gaps for A.C. Systems*, document BS EN 60099-4, 2004.

[22] *IEEE Guide for the Application of Metal Oxide Surge Arresters for Alternating-Current Systems*, IEEE Standard C62.22-1, 1991.

[23] J. Lundquist, L. Stenstrom, A. Schei, and B. Hansen, "New method for measurement of the resistive leakage currents of metal-oxide surge arresters in service," *IEEE Trans. Power Del.*, vol. 5, no. 4, pp. 1811–1822, Oct. 1990.

[24] C. Heinrich and V. Hinrichsen, "Diagnostics and monitoring of metal-oxide surge arresters in high-voltage networks-comparison of existing and newly developed procedures," *IEEE Trans. Power Del.*, vol. 16, no. 1, pp. 138–143, Jan. 2001.

[25] *ABB EXCOUNT-II User's Manual*, document 1HSA 801 080-15 Edition 3.2, 2010-03. 2010. [Online]. Available: http://new.abb.com/high-voltage/surge-arresters/high-voltage-arresters/surge-counters-and-monitors-for-surge-arresters-accessories/excount-ii

[26] *Doble Lemke LCM 500 Leakage Current Monitor*, accessed on Jun. 16, 2016. [Online]. Available: http://www.doble.com/product/lcm500/

[27] E. Fontana, S. C. Oliveira, F. J. M. M. Cavalcanti, R. B. Lima, J. F. Martins-Filho, and E. Meneses-Pacheco, "Novel sensor system for leakage current detection on insulator strings of overhead transmission lines," *IEEE Trans. Power Del.*, vol. 21, no. 4, pp. 2064–2070, Oct. 2006.

[28] S. Kurihara *et al.*, "Construction of remote monitoring system for separative measurement of leakage current of outdoor insulators," in *Proc. IEEE 7th Int. Conf. Properties Appl. Dielectr. Mater.*, vol. 1. Nagoya, Japan, 2003, pp. 401–404.

[29] S. Shihab, V. Melik, L. Zhou, G. Melik, and N. Alame, "On-line pollution leakage current monitoring system," in *Proc. 4th Int. Conf. Properties Appl. Dielectr. Mater.*, vol. 2. Brisbane, QLD, Australia, 1994, pp. 538–541.

[30] *Artificial Pollution Tests on High-Voltage Insulators to be Used on AC Systems*, document BSEN 60507, British Standards Institution, 1993.

[31] D. Guo, U. Hauser-Ehninger, H. Griffiths, A. Haddad, A. Ainsley, F. Ainslie and D. Frame, "A technique for the continuous condition monitoring of substation earthing systems," in *Proc. 15th Int. Symp. High Voltage Eng. (ISH)*, Ljubljana, Slovenia, Aug. 2007, pp. 1–6, paper T2-445.

[32] Riverbed Technology, San Francisco, CA, USA. (2010). *Riverbed AirPCap Datasheet*. [Online]. Available: www.riverbed.com/document/fpo/DataSheet-Riverbed-AirPcap.pdf

[33] MetaGeek Tech. Ltd., Canada. (2016). *Wy-Spy 2.4x Datasheet*. [Online]. Available: http://www.wispy.ca/wyspi24x.php

N. HARID (M'13) received the Ph.D. degree in electrical engineering from the University of Wales, Cardiff, U.K. He was an Associate Professor for several years before joining the High-Voltage Energy Systems Group, Cardiff University, Cardiff, in 2001, as a Senior Researcher and Senior Lecturer. In 2013, he joined the Petroleum Institute, Abu Dhabi, where he is an Associate Professor of Electric Power and High-Voltage Engineering. He has authored or co-authored over 100 publications in his areas of research. His main research interests are in earthing systems, insulation systems, transients, breakdown phenomena, and monitoring of high-voltage plant. He is a member of the IET and a fellow of the Higher Education Academy and served as a member of the BSI GEL/81 Standard Committee on Lightning Protection.

A. C. BOGIAS received the B.Eng. degree in electrical and electronic engineering in 2004, and the Ph.D. degree from Cardiff University in 2012.

H. GRIFFITHS (M'15) received the B.Sc. degree in 1982, and received the Ph.D. degree from Cardiff University, U.K. From 1983 to 1990, he was with the South Wales Electricity Board and the Central Electricity Generating Board, where he was an Engineer in distribution and transmission system design. In 1990, he was appointed as a Lecturing Staff Member with Cardiff University. Since 2015, he has been a Professor of Power systems and High-Voltage Engineering with the Petroleum Institute, Abu Dhabi, prior to that with Cardiff University. His research interests include earthing systems and transients. He is currently a member of British Standard Institution Committees BSI PEL/99 (HV ac substations), the Chair of BSI GEL/600 (earthing), and a member of CENELEC TC99X WG1, Earthing of Power Installations exceeding 1-kV ac, and the IEC Committee TC99/MT4-IEC 61936 Power Installations exceeding 1-kV ac. He is a Chartered Engineer and a member of the IET.

S. ROBSON (M'13) received the M.Eng. degree in 2007 and the Ph.D. degree in 2012. In 2013, he was appointed as Lecturer in Electrical Engineering with Cardiff University. His main research interests are power line communication, fault location, condition monitoring, and simulation of transients on electrical networks.

A. HADDAD (M'13) received the degree of Ingénieur d'État in electrical engineering in 1985 and the Ph.D. degree in high-voltage engineering in 1990. He is currently a Professor of Electrical Engineering with Cardiff University with responsibility for research in high-voltage engineering. He has authored an IET-Power Series Book entitled *Advances in High-Voltage Engineering*. His research interests are in overvoltage protection, insulation systems, insulation coordination, and earthing of electrical energy systems. He is a member of CIGRE Working Groups and a member of the BSI PEL1/2, the IEC TC37, and the IEC ACTAD committees. He serves on the scientific committees of several international conferences. He is a fellow of the IET and the Learned Society of Wales.